Generation of a Maximally Entangled State Using Collective Optical Pumping

M. Malinowski[1,*] C. Zhang[1], V. Negnevitsky,[1] I. Rojkov[1], F. Reiter[1], T.-L. Nguyen[1],
M. Stadler[1], D. Kienzler[1], K. K. Mehta,[1] and J. P. Home[1,2,†]

[1]*Institute for Quantum Electronics, ETH Zürich, 8093 Zürich, Switzerland*
[2]*Quantum center, ETH Zürich, 8093 Zürich, Switzerland*

We propose and implement a novel scheme for dissipatively pumping two qubits into a singlet Bell state. The method relies on a process of collective optical pumping to an excited level, to which all states apart from the singlet are coupled. We apply the method to deterministically entangle two trapped ^{40}Ca$^+$ ions. Within 16 pumping cycles, an initially separable state is transformed into one with 83(1)% singlet fidelity, and states with initial fidelity of $\gtrsim$ 70% converge onto a fidelity of 93(1)%. We theoretically analyze the performance and error susceptibility of the scheme and find it to be insensitive to a large class of experimentally relevant noise sources.

Quantum entanglement is a resource for quantum computation [1], communication [2], cryptography [3], and metrology [4]. Entangled states are typically prepared using a two-step process, the first involving initialization of a separable state by optical pumping, followed by a unitary transformation which generates entanglement [5]. In such an *open-loop process* the final state is sensitive to the parameters of the drive used to create it and is not protected from future errors. An alternative mode of operation is to use a *closed-loop process*, where feedback from a low-entropy reference system drives the system continuously toward the desired state or subspace. This can be done using measurement-conditioned classical control (e.g., quantum error correction or outcome heralding) or through dissipative engineering [6–10]. Dissipation engineering allows useful quantum states to be created in the steady state, making the process self-correcting with regard to transient errors [11,12], and resulting in a resource state or subspace which is continuously available. Entanglement of qubits using dissipative engineering has previously been demonstrated using trapped ions [13,14], atomic ensembles [15], and superconducting circuits [16–18]. Beyond qubit-based approaches, reservoir engineering has been used to create and stabilize nonclassical states of bosonic systems [6,19,20] as well as to perform quantum error correction [20,21].

A widely used strategy for dissipation engineering is to rely on engineered resonances, whereby pumping into the desired entangled state is achieved by resonant drives,

while leakage processes out of the desired state are off resonant [11,14,22,23]. This approach has proven to be versatile, and has been theoretically extended to the generation of multiqubit states [24–26], quantum error correction [27,28], and quantum simulation [29]. However, these protocols can be slow to converge. This is because, in order to suppress leakage processes, the drives need to be weak compared to the splittings of the resonances. The resulting competition with additional uncontrolled dissipation channels limits the achievable fidelities. It has been proposed that this issue could be overcome by dissipative schemes based on symmetry [30–34].

In this Letter, we present a method for dissipatively generating two-body entanglement using a deterministic collective optical pumping process which does not couple to the target entangled state: the singlet Bell state $|\Psi^-\rangle \equiv (|\uparrow\downarrow\rangle - |\downarrow\uparrow\rangle)/\sqrt{2}$. Unlike previous demonstrations, our method relies on symmetry, involving only global fields which couple equally to each system. We thereby overcome the speed limitations of previous schemes, achieving a faster convergence. Our scheme is robust to global error processes. We implement the protocol using two trapped ions in a surface-electrode trap with integrated optical control fields [35], achieving a 93(1)% fidelity with $|\Psi^-\rangle$. Compared to earlier trapped-ion approaches, our method does not require ground-state cooling.

The scheme is illustrated in Fig. 1(a). We consider a spin ground-state manifold consisting of the collective states $|\downarrow\downarrow\rangle, |\uparrow\uparrow\rangle, |\Psi^+\rangle \equiv (|\uparrow\downarrow\rangle + |\downarrow\uparrow\rangle)/\sqrt{2}$ (spin triplet) and $|\Psi^-\rangle$ (spin singlet), as well as excited states, of which the most important for our purposes consists of both systems in a particular excited state $|e\rangle$. Three elements define the pumping process. The first is a collective excitation (A) from $|\downarrow\downarrow\rangle$ to $|ee\rangle$. Its collective nature
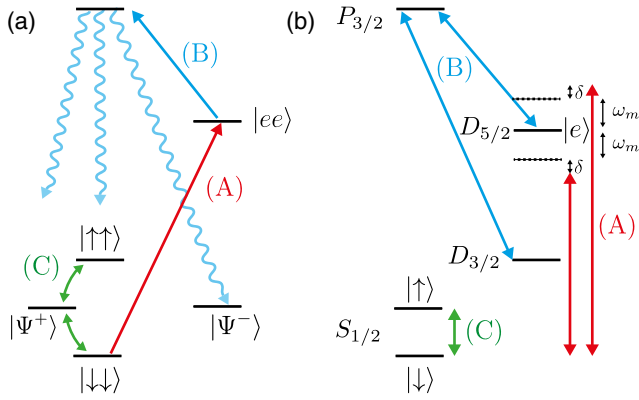
FIG. 1. (a) High-level description of the protocol. When drives (A), (B), and (C) are switched on, the system is pumped into a maximally entangled state $|\Psi^-\rangle$. (b) Atomic transitions and drives in $^{40}Ca^+$ used in this work. (A) and (B) are driven by laser beams, while (C) is implemented by an oscillating B field. Dashed lines denote motional sidebands of the $|\downarrow\rangle \leftrightarrow |e\rangle$ transition.

means that it does not couple to the other states in the ground-state manifold. The state $|ee\rangle$ is quenched through a decay channel (B), redistributing its population into all four spin states. (A) and (B) together provide a collective optical pumping process which moves the population from $|\downarrow\downarrow\rangle$ to the other ground states. To prepare only the singlet, this is supplemented by a symmetric drive (C) which resonantly drives both spins with equal amplitude and phase. Because of its symmetry, this drive cycles population within the triplet subspace, while leaving the singlet untouched. Thus the triplet states have a chance of being repumped through the collective pumping, while population in the singlet is dark to all drives. $|\Psi^-\rangle$ then becomes the steady state of the system. The protocol can be implemented continuously or by sequentially applying each component. For our implementation, we expect the latter to be more robust to experimental imperfections and analyze it below. The continuous implementation is analyzed in detail in Supplemental Material (SM), Sec. VI [36].

To identify optimal settings, we optimize a superoperator which combines the three drives. For the collective excitation this is derived from a unitary,

$$U_A(\Phi) = e^{-i\Phi S_{x,e}^2}, \quad (1)$$

with $S_{x,e} = \sigma_{x,\downarrow e} \otimes 1 + 1 \otimes \sigma_{x,\downarrow e}$, $\sigma_{x,\downarrow e} = |e\rangle\langle\downarrow| + |\downarrow\rangle\langle e|$, and 1 is a 3×3 identity operator. This provides a full transfer from $|\downarrow\downarrow\rangle$ to $|ee\rangle$ for $\Phi = \pi/4$. Drive (B) repumps the population from $|e\rangle$ with branching ratios parametrized by $p_{e\to\downarrow}/p_{e\to\uparrow} = \tan^2(\gamma)$. Drive (C) is described by a unitary $U_C(\theta) = \exp[i(\theta/2)\sigma_x] \otimes \exp[i(\theta/2)\sigma_x]$, where $\sigma_x = |\uparrow\rangle\langle\downarrow| + |\downarrow\rangle\langle\uparrow|$. After $N \gg 1$ cycles, the singlet fidelity, defined as $F(|\Psi^-\rangle) = \langle\Psi^-|\rho|\Psi^-\rangle$ for the system density matrix ρ, approaches unity as $F(|\Psi^-\rangle) \propto$

$1 - \exp(-N/N_0)$. Through eigenvalue analysis we find the most rapid convergence for $\Phi = \pi/4$, $\theta \approx 0.72\pi$, and $\gamma \approx 0.22\pi$, where $N_0 = 7.62$ cycles (SM, Sec. I [36]). The steady state is insensitive to the values of Φ, γ, and θ, indicating that these parameters do not require precise calibration.

We implement the protocol on a pair of $^{40}Ca^+$ ions confined in the surface-electrode trap described in Ref. [35]. The qubit is encoded into ground-state Zeeman sublevels $|\downarrow\rangle = |S_{1/2}, m_j = -1/2\rangle$ and $|\uparrow\rangle = |S_{1/2}, m_j = +1/2\rangle$ which have a frequency splitting of $2\pi \times 16.5$ MHz in the applied magnetic field of 0.59 mT. We use an ancilliary state $|e\rangle = |D_{5/2}, m_j = -1/2\rangle$. Narrow-linewidth laser light at 729 nm is delivered through trap-integrated photonics, and coherently drives the $S_{1/2} \leftrightarrow D_{5/2}$ transitions. Free-space laser beams are used for cooling, repumping, and readout. The $|\downarrow\rangle \leftrightarrow |\uparrow\rangle$ transition is driven by resonant radio-frequency magnetic fields.

The collective excitation step (A) is implemented using a bichromatic 729 nm laser field with Rabi frequency Ω and two frequency components detuned by $\delta = \pm 2\pi \times 14.7$ kHz from the red and blue motional sidebands of the $|\downarrow\rangle \leftrightarrow |e\rangle$ transition, using the axial stretch mode (where ions oscillate out of phase) at $\omega_m \approx 2\pi \times 2.4$ MHz for which the Lamb-Dicke parameter $\eta = 0.026$. This results in a Hamiltonian $H_A = \frac{1}{2}\hbar\eta\Omega S_{x,e}(\hat{a}e^{i\delta t} + \hat{a}^\dagger e^{-i\delta t})$ which implements a force on the oscillator whose phase depends on the eigenstate of $S_{x,e}$. This is commonly referred to as a Mølmer-Sørensen drive, and is one of the primary methods for performing two-qubit gates with trapped ions [37–39]. A pulse of duration t then results in the unitary

$$U_A = e^{[\alpha(t)\hat{a}^\dagger - \alpha^*(t)\hat{a}]S_{x,e}} e^{i\Phi(t)S_{x,e}^2}, \quad (2)$$

where $\alpha(t) = -i(\eta\Omega/\delta)e^{-i\delta t/2}\sin(\delta t/2)$ is an oscillator phase-space displacement amplitude and $\Phi(t) = (\eta^2\Omega^2/4\delta^2)[\delta t - \sin(\delta t)]$ is a collective phase factor. Equation (2) reduces to a pure $S_{x,e}^2$ coupling of the form of Eq. (1) in two cases. The first, appropriate to a continuous implementation, is when $|\delta| \gg \eta\Omega$ and so the oscillator excitation can be neglected [40]. The second, which is the main focus of this Letter, is when $t = 2n\pi/\delta$ with $n \in \mathbb{Z}$, for which $\Phi = n\pi\eta^2\Omega^2/(2\delta^2)$ [41]. Repump (B) is implemented using a laser at 854 nm, which couples all $D_{5/2}$ sublevels to the short-lived $P_{3/2}$ states, which primarily decay into the ground-state manifold. A second decay channel to the $D_{3/2}$ states is repumped using a laser at 866 nm. After 5 μs, we measure a probability of leaving $D_{5/2}$ of > 0.9999 with a branching ratio of $\gamma \simeq 0.3\pi$. The symmetric drive (C) is implemented by passing a current through a track on a circuit board at around 1 mm distance from the ions.

We employ a number of error mitigation techniques. The collective excitation step (A) is implemented as a sequence of two pulses ($t = 2n\pi/\delta$ with $n = 2$) with $\eta\Omega = \delta/2$, resulting in $\Phi = \pi/4$ and a drive time of $t = 150$ μs.

The phase of the force acting on the oscillator is shifted by π for the second pulse, thus canceling any residual displacement produced by a single pulse [42]. To our surprise the ac Stark shift of the $|\downarrow\rangle \leftrightarrow |\uparrow\rangle$ transition produced by the collective drive was different by $\approx 2\pi \times 2.5$ kHz on the two ions, causing a near-complete failure of the protocol (SM, Sec. IV [36]). To mitigate this, we replace the optimal value of θ applied in each cycle with two values, $\theta_1 = \pi$ applied in odd cycles (drive time $t_C = 6.4\ \mu s$) and $\theta = \pi/2$ ($t_C = 3.2\ \mu s$) applied in even cycles. This has the desired effect of a spin echo, but at the cost that high-fidelity singlet states are produced only after even cycles. One cycle of the protocol takes $\approx 165\ \mu s$ on average. In the absence of other errors, the protocol produces $|\Psi^-\rangle$ regardless of the ions' temperature. However, finite temperature amplifies existing errors associated with residual oscillator excitation [i.e., when $|\alpha(t)| > 0$]. For this reason, we cool the ion close to the motional ground state.

We measure the $P(\downarrow\downarrow)$, $P(\downarrow\uparrow) + P(\uparrow\downarrow)$, and $P(\uparrow\uparrow)$ populations by shelving $|\downarrow\rangle$ into ancillary $D_{5/2}$ sublevels, followed by state-dependent fluorescence [43]. This allows us to extract the ground-state parity $\langle\sigma_z\sigma_z\rangle$, while $\langle\sigma_x\sigma_x\rangle$ and $\langle\sigma_y\sigma_y\rangle$ are obtained by measuring the parity following radio-frequency spin rotations $\exp[i(\pi/2)\sigma_x] \otimes \exp[i(\pi/2)\sigma_x]$ and $\exp[i(\pi/2)\sigma_y] \otimes \exp[i(\pi/2)\sigma_y]$, respectively. These are combined to estimate the singlet state fidelity, using $F(|\Psi^-\rangle) = \frac{1}{4}(1 - \langle\sigma_x\sigma_x\rangle - \langle\sigma_y\sigma_y\rangle - \langle\sigma_z\sigma_z\rangle)$.

Figure 2(a) shows the measured fidelity as a function of the number of cycles of the protocol, applied to a range of initial states, showing the expected convergence toward the singlet. Different starting states were created by initializing the ions to $|\downarrow\downarrow\rangle$ and mapping it to a mixture of singlet and triplet states (SM. Sec. V [36]). Figure 2(b) illustrates how, after 16 cycles of the protocol, states with initial fidelities $\gtrsim 0.75$ are mapped onto output states with the same final fidelity. Averaged over all the data, we find a fidelity of 93(1)% at 16 cycles.

We analyze the noise robustness of the protocol by considering the bichromatic drive (A) as the dominant source of errors. Assuming $|\uparrow\rangle$ is spectroscopically decoupled from (A), we can describe all errors through 16 elementary error channels $\{I_e, X_e, Y_e, Z_e\}^{\otimes 2}$. These act as Pauli operators on the $\{|\downarrow\rangle, |e\rangle\}$ subspace, and as identity on $|\uparrow\rangle$ (SM, Sec. II [36]). The effect of those errors acting with probability p per cycle in a depolarizing model is shown in Fig. 3(a). We find that the final fidelity is independent of all global errors (such as X_eX_e or X_eZ_e). On the other hand, all local errors (such as X_eI_e or I_eZ_e) become amplified. A particularly experimentally relevant class of errors is *correlated local errors*. These include correlated bit-flip errors (corresponding to an application of the operator $I_eX_e + X_eI_e$) which arise due to residual spin-motion entanglement at the end of the collective excitation step [i.e., when $\alpha(t) \neq 0$] or off-resonant excitation of
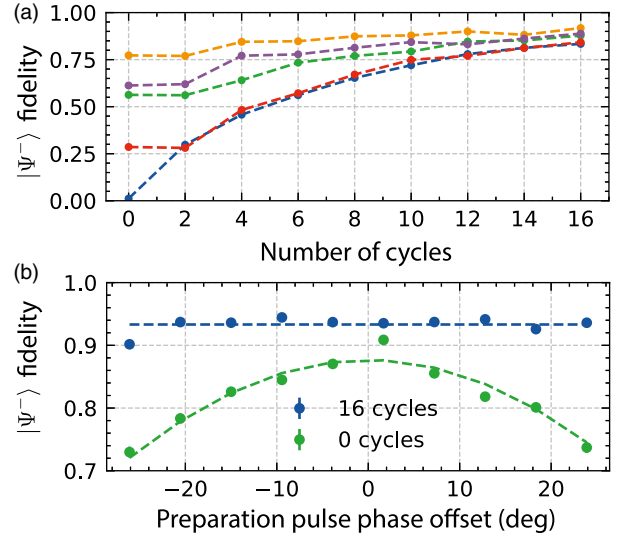

FIG. 2. Entanglement generation. (a) The effect of applying up to 16 cycles of the protocol. Measurements for different initial states are shown in different colors and connected by dashed lines. All cases converge toward $|\Psi^-\rangle$. (b) Comparison of the singlet fidelity before and after the protocol is applied. The phase ϕ_{prep} of the preparation pulse (SM, Sec. V [36]) sets the input fidelity to $F(|\Psi^-\rangle) \approx 0.88\cos^2\phi_{prep}$ (green dashed line). After 16 cycles, states with fidelities $\gtrsim 0.75$ converge onto the same state of $F(|\Psi^-\rangle) \approx 0.93$ (blue dashed line). Statistical $\pm 1\sigma$ error bars are smaller than data points, and the result spread is dominated by experimental drifts.

"spectator" transitions (i.e., nearby undesired resonances). Magnetic-field fluctuations common to both ions would produce a correlated phase-flip error ($I_eZ_e + Z_eI_e$). We find that such correlations increase the fidelity of the collective optical pumping compared with uncorrelated errors with similar constituent operators. Results of simulations showing this are displayed in Fig. 3(b). For example, a bit-flip error with probability p per cycle reduces the singlet fidelity by $\approx 5.2p$ when uncorrelated and $\approx 3.2p$ when correlated. Correlated phase-flip errors leave the fidelity unaffected since $|\Psi^-\rangle$ resides in a decoherence-free subspace.

These insights are matched by simulations of the dynamics of the collective optical pumping in the presence of experimentally relevant error sources. These reveal that, compared to either a single entangling gate or a two-loop phase-modulated entangling gate [44] based on the Hamiltonian H_A, our protocol reduces the effect of qubit frequency errors and Rabi frequency errors. For motional frequency errors and fast (Markovian) optical qubit dephasing, our protocol does not provide benefits. Details and discussion of practical applicability of these results are presented in SM, Sec. III [36].

It is challenging to exactly account for the measured error from first principles due to a number of setup-specific imperfections. We experience kilohertz-level drifts in
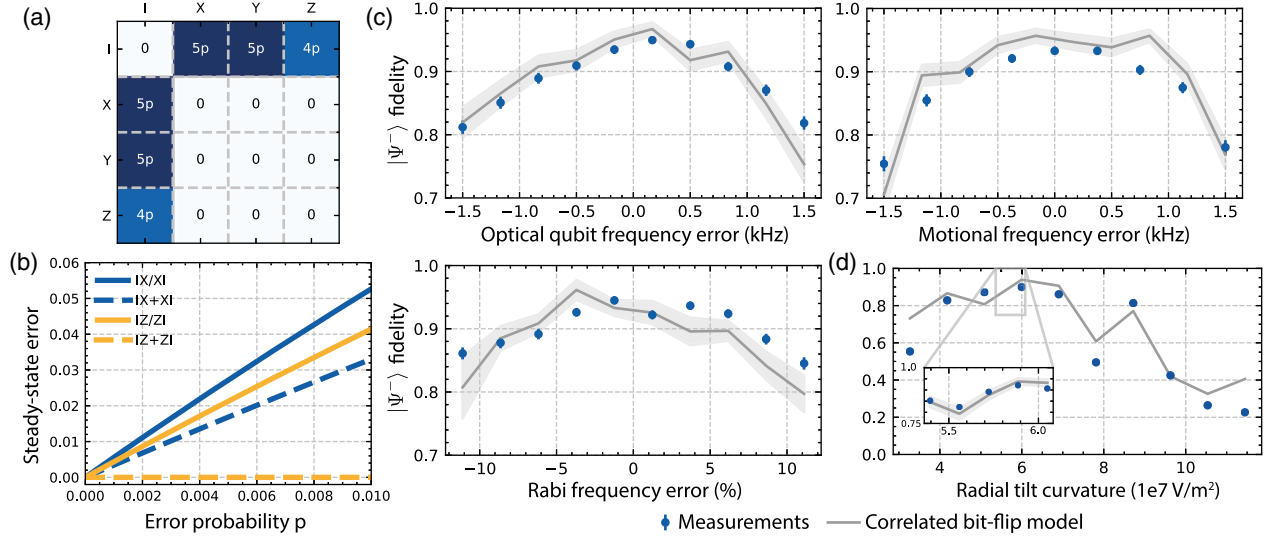
FIG. 3. (a) Simulated steady-state error associated with individual error channels of probability p. (b) Comparison of simulated steady-state errors associated with uncorrelated (solid lines) and correlated (dashed lines) errors. (c),(d) Experimentally measured values of $F(|\Psi^-\rangle)$ (blue dots) compared to the prediction $(1 - 3.2p)$ of a correlated bit-flip error model (gray lines), with p obtained from independent experimental measurements. Error bars (smaller than most data points) show a $\pm 1\sigma$ confidence interval. In several data points in (d) the measured values of p are large, and we can no longer apply the linear approximation. Inset in (d) highlights the typical operation region

motional mode frequencies due to charging of the trap surface by light shining through the integrated waveguides [45]. These occasionally lead to a mode spectrum where the collective excitation step off-resonantly excites spectator optical transitions. This error can be corrected by tuning mode frequencies, but it is challenging to estimate its magnitude between calibrations. Mode frequency drifts associated with laser power changes were also the primary reason we worked with a fixed number of protocol cycles ($N = 16$, corresponding to ≈ 3 ms of 729 nm light per shot). High heating rates mean that each cycle of the protocol starts with a higher occupancy of motional modes (≈ 0.5 quanta per cycle on a 1 MHz center-of-mass mode), leading to an increase in a correlated bit-flip error during the drive (A) as the protocol progresses. The combined effect of all the error sources is a bit-flip error probability of $p \approx 0.01$ for the first cycle, and $p \approx 0.02$ after 16 cycles. The measured 16-cycle fidelity 93(1)% is consistent with the value of $1 - 3.2p$ predicted by the correlated bit-flip error model. The obtained fidelity is significantly reduced compared to the unitary gate based on the same Hamiltonian H_A, which produces $(|\downarrow\downarrow\rangle - i|ee\rangle)/\sqrt{2}$ with fidelity of $\gtrsim 99\%$ [35], though it does improve our ability to prepare $|\Psi^-\rangle$, which is currently limited by errors in single-ion addressing in our coherent implementation.

In order to verify that the correlated bit-flip error model captures the essential performance limitations of the protocol, we measure the 16-cycle fidelity, as well as the bit-flip probability in the collective excitation step, for a range of experimental miscalibrations. For each parameter,

we experimentally approximate the steady-state fidelity $F(|\Psi^-\rangle)$ by first preparing $|\Psi^-\rangle$ with fidelity around 0.75 using unitary methods, and then applying 16 cycles of the protocol. The bit-flip probability p for the last cycle is independently estimated by applying 16 cycles of the protocol, followed by optical pumping and a single round of drive (A) (SM, Sec. V [36]). The comparison between ; $F(|\Psi^-\rangle)$ and the bit-flip model prediction is shown in Fig. 3(c). We find qualitative agreement, suggesting that the bit-flip model accurately captures the errors of the protocol. Figure 3(d) illustrates the challenge associated with spectral crowding. We modify the spectator mode spectrum by adding an additional quadrupole potential with eigenaxes at $\pm 45°$ to the trap surface in the radial plane. This changes the radial mode orientations, frequencies, and temperatures, while keeping the (axial) gate mode frequency approximately constant. We find that the spectator spectrum is clear only for a narrow range of curvatures (here between 5.7×10^7 and 6.1×10^7 V/m^2), which needs recalibrating every few hours.

All of the limitations listed above are setup specific and do not pose a fundamental limitation to the protocol. Coupling to spectator transitions could be suppressed by increasing the magnetic field. The heating rate observed in this trap is particularly high, exceeding levels observed in cryogenic traps with comparable ion-electrode distances by a factor of ≈ 100 [46,47]. Reducing it to more typical levels, combined with better shielding of nearby dielectrics [48,49], would suppress drifts within each collective pumping sequence and hence allow the protocol to reach

its true steady state. Alternatively, motional mode temperature could be stabilized throughout the protocol by sympathetic cooling [50].

We have presented and implemented a novel protocol for collective optical pumping into a maximally entangled two-qubit state. We measure a singlet fidelity of 93(1)% after 16 cycles of the protocol (at which point a quasisteady state has been achieved), to our knowledge exceeding previously reported dissipative methods, and slightly below a simultaneous work by Cole *et al.* [34]. The observed infidelity is consistent with measured bit-flip errors of the effective S_x^2 drive which for our implementation is mediated by a motional mode. The protocol can be practically beneficial in experiments limited by global errors, especially as a method of purifying lower-fidelity Bell states. Dissipative generation of high-fidelity entangled states could find application in a variety of quantum information processing tasks, such as dissipative encoding [51], error-corrected quantum sensing [52], and as a supply of entangled resource states for quantum gate teleportation [53].

While the analysis in this Letter focused on a specific implementation in $^{40}\text{Ca}^+$ ions, the protocol is general, and we anticipate it might be applied in a wide range of platforms where collective excitation may be engineered. These include nitrogen-vacancy centers (via direct spin-spin interactions [54]), neutral atom platforms (via Rydberg dressing [55]) or superconductors (via parametric drives [32]).

---

[*] maciejm@phys.ethz.ch
[†] jhome@phys.ethz.ch

[1] R. Jozsa and N. Linden, On the role of entanglement in quantum-computational speed-up, Proc. R. Soc. A **459**, 2011 (2003).

[2] C. H. Bennett and S. J. Wiesner, Communication via One- and Two-Particle Operators on Einstein-Podolsky-Rosen States, Phys. Rev. Lett. **69**, 2881 (1992).

[3] A. K. Ekert, Quantum Cryptography Based on Bell's Theorem, Phys. Rev. Lett. **67**, 661 (1991).

[4] G. Tóth and I. Apellaniz, Quantum metrology from a quantum information science perspective, J. Phys. A **47**, 424006 (2014).

[5] D. P. DiVincenzo, The physical implementation of quantum computation, Fortschr. Phys. **48**, 771 (2000).

[6] J. F. Poyatos, J. I. Cirac, and P. Zoller, Quantum Reservoir Engineering with Laser Cooled Trapped Ions, Phys. Rev. Lett. **77**, 4728 (1996).

[7] B. Kraus, H. P. Büchler, S. Diehl, A. Kantian, A. Micheli, and P. Zoller, Preparation of entangled states by quantum Markov processes, Phys. Rev. A **78**, 042307 (2008).

[8] M. B. Plenio, S. F. Huelga, A. Beige, and P. L. Knight, Cavity-loss-induced generation of entangled atoms, Phys. Rev. A **59**, 2468 (1999).

[9] F. Verstraete, M. M. Wolf, and J. Ignacio Cirac, Quantum computation and quantum-state engineering driven by dissipation, Nat. Phys. **5**, 633 (2009).

[10] F. Ticozzi and L. Viola, Steady-state entanglement by engineered quasi-local Markovian dissipation, Quantum Inf. Comput. **14**, 265 (2014).

[11] M. J. Kastoryano, F. Reiter, and A. S. Sørensen, Dissipative Preparation of Entanglement in Optical Cavities, Phys. Rev. Lett. **106**, 090502 (2011).

[12] G. Morigi, J. Eschner, C. Cormick, Y. Lin, D. Leibfried, and D. J. Wineland, Dissipative Quantum Control of a Spin Chain, Phys. Rev. Lett. **115**, 200502 (2015).

[13] J. T. Barreiro, M. Müller, P. Schindler, D. Nigg, T. Monz, M. Chwalla, M. Hennrich, C. F. Roos, P. Zoller, and R. Blatt, An open-system quantum simulator with trapped ions, Nature (London) **470**, 486 (2011).

[14] Y. Lin, J. P. Gaebler, F. Reiter, T. R. Tan, R. Bowler, A. S. Sørensen, D. Leibfried, and D. J. Wineland, Dissipative production of a maximally entangled steady state of two quantum bits, Nature (London) **504**, 415 (2013).

[15] H. Krauter, C. A. Muschik, K. Jensen, W. Wasilewski, J. M. Petersen, J. I. Cirac, and E. S. Polzik, Entanglement Generated by Dissipation and Steady State Entanglement of Two Macroscopic Objects, Phys. Rev. Lett. **107**, 080503 (2011).

[16] S. Shankar, M. Hatridge, Z. Leghtas, K. M. Sliwa, A. Narla, U. Vool, S. M. Girvin, L. Frunzio, M. Mirrahimi, and M. H. Devoret, Autonomously stabilized entanglement between two superconducting quantum bits, Nature (London) **504**, 419 (2013).

[17] Y. Liu, S. Shankar, N. Ofek, M. Hatridge, A. Narla, K. M. Sliwa, L. Frunzio, R. J. Schoelkopf, and M. H. Devoret, Comparing and Combining Measurement-Based and Driven-Dissipative Entanglement Stabilization, Phys. Rev. X **6**, 011022 (2016).

[18] M. E. Kimchi-Schwartz, L. Martin, E. Flurin, C. Aron, M. Kulkarni, H. E. Tureci, and I. Siddiqi, Stabilizing Entanglement via Symmetry-Selective Bath Engineering in Superconducting Qubits, Phys. Rev. Lett. **116**, 240503 (2016).

[19] D. Kienzler, H. Y. Lo, V. Negnevitsky, C. Flühmann, M. Marinelli, and J. P. Home, Quantum Harmonic Oscillator State Control in a Squeezed Fock Basis, Phys. Rev. Lett. **119**, 033602 (2017).

[20] B. de Neeve, T. L. Nguyen, T. Behrle, and J. Home, Error correction of a logical grid state qubit by dissipative pumping, arXiv:2010.09681.

[21] J. M. Gertler, B. Baker, J. Li, S. Shirol, J. Koch, and C. Wang, Protecting a bosonic qubit with autonomous quantum error correction, Nature (London) **590**, 243 (2021).

[22] G. Vacanti and A. Beige, Cooling atoms into entangled states, New J. Phys. **11**, 083008 (2009).

[23] F. Reiter and A. S. Sørensen, Effective operator formalism for open quantum systems, Phys. Rev. A **85**, 032111 (2012).

[24] J. Cho, S. Bose, and M. S. Kim, Optical Pumping into Many-Body Entanglement, Phys. Rev. Lett. **106**, 020504 (2011).

[25] Y. Lin, J. P. Gaebler, F. Reiter, T. R. Tan, R. Bowler, Y. Wan, A. Keith, E. Knill, S. Glancy, K. Coakley, A. S. Sørensen, D. Leibfried, and D. J. Wineland, Preparation of Entangled States through Hilbert Space Engineering, Phys. Rev. Lett. **117**, 140502 (2016).

[26] F. Reiter, D. Reeb, and A. S. Sørensen, Scalable Dissipative Preparation of Many-Body Entanglement, Phys. Rev. Lett. **117**, 040501 (2016).

[27] J. Cohen and M. Mirrahimi, Dissipation-induced continuous quantum error correction for superconducting circuits, Phys. Rev. A **90**, 062344 (2014).

[28] F. Reiter, A. S. Sørensen, P. Zoller, and C. A. Muschik, Dissipative quantum error correction and application to quantum sensing with trapped ions, Nat. Commun. **8**, 1 (2017).

[29] F. Reiter, F. Lange, S. Jain, M. Grau, J. P. Home, and Z. Lenarčič, Engineering generalized Gibbs ensembles with trapped ions, Phys. Rev. Research **3**, 033142 (2021).

[30] C. D. B. Bentley, A. R. R. Carvalho, D. Kielpinski, and J. J. Hope, Detection-Enhanced Steady State Entanglement with Ions, Phys. Rev. Lett. **113**, 040501 (2014).

[31] K. P. Horn, F. Reiter, Y. Lin, D. Leibfried, and C. P. Koch, Quantum optimal control of the dissipative production of a maximally entangled state, New J. Phys. **20**, 123010 (2018).

[32] E. Doucet, F. Reiter, L. Ranzani, and A. Kamal, High fidelity dissipation engineering using parametric interactions, Phys. Rev. Research **2**, 023370 (2020).

[33] D. C. Cole, J. J. Wu, S. D. Erickson, P.-Y. Hou, A. C. Wilson, D. Leibfried, and F. Reiter, Dissipative preparation of W states in trapped ion systems, New J. Phys. **23**, 073001 (2021).

[34] D. C. Cole, S. D. Erickson, G. Zarantonello, K. P. Horn, P.-Y. Hou, J. J. Wu, D. H. Slichter, F. Reiter, C. P. Koch, and D. Leibfried, preceding Letter, Resource-Efficient Dissipative Entanglement of Two Trapped-Ion Qubits, Phys. Rev. Lett. **128**, 080502 (2022).

[35] K. K. Mehta, C. Zhang, M. Malinowski, T. L. Nguyen, M. Stadler, and J. P. Home, Integrated optical multi-ion quantum logic, Nature (London) **586**, 533 (2020).

[36] See Supplemental Material at http://link.aps.org/supplemental/10.1103/PhysRevLett.128.080503 for extended discussion of the protocol and the experiment.

[37] A. Sørensen and K. Mølmer, Quantum Computation with Ions in Thermal Motion, Phys. Rev. Lett. **82**, 1971 (1999).

[38] J. Benhelm, G. Kirchmair, C. F. Roos, and R. Blatt, Towards fault-tolerant quantum computing with trapped ions, Nat. Phys. **4**, 463 (2008).

[39] J. P. Gaebler, T. R. Tan, Y. Lin, Y. Wan, R. Bowler, A. C. Keith, S. Glancy, K. Coakley, E. Knill, D. Leibfried, and D. J. Wineland, High-Fidelity Universal Gate Set for ^{9}Be$^+$ Ion Qubits, Phys. Rev. Lett. **117**, 060505 (2016).

[40] K. Kim, M. S. Chang, S. Korenblit, R. Islam, E. E. Edwards, J. K. Freericks, G. D. Lin, L. M. Duan, and C. Monroe, Quantum simulation of frustrated Ising spins with trapped ions, Nature (London) **465**, 590 (2010).

[41] G. Kirchmair, J. Benhelm, F. Zähringer, R. Gerritsma, C. F. Roos, and R. Blatt, Deterministic entanglement of ions in thermal states of motion, New J. Phys. **11**, 023002 (2009).

[42] D. Hayes, S. M. Clark, S. Debnath, D. Hucul, I. V. Inlek, K. W. Lee, Q. Quraishi, and C. Monroe, Coherent Error Suppression in Multiqubit Entangling Gates, Phys. Rev. Lett. **109**, 020503 (2012).

[43] A. H. Myerson, D. J. Szwer, S. C. Webster, D. T. C. Allcock, M. J. Curtis, G. Imreh, J. A. Sherman, D. N. Stacey, A. M. Steane, and D. M. Lucas, High-Fidelity Readout of Trapped-Ion Qubits, Phys. Rev. Lett. **100**, 200502 (2008).

[44] A. R. Milne, C. L. Edmunds, C. Hempel, F. Roy, S. Mavadia, and M. J. Biercuk, Phase-Modulated Entangling Gates Robust to Static and Time-Varying Errors, Phys. Rev. Applied **13**, 024022 (2020).

[45] M. Harlander, M. Brownnutt, W. Hänsel, and R. Blatt, Trapped-ion probing of light-induced charging effects on dielectrics, New J. Phys. **12**, 093035 (2010).

[46] M. Brownnutt, M. Kumph, P. Rabl, and R. Blatt, Ion-trap measurements of electric-field noise near surfaces, Rev. Mod. Phys. **87**, 1419 (2015).

[47] J. A. Sedlacek, J. Stuart, D. H. Slichter, C. D. Bruzewicz, R. McConnell, J. M. Sage, and J. Chiaverini, Evidence for multiple mechanisms underlying surface electric-field noise in ion traps, Phys. Rev. A **98**, 063430 (2018).

[48] S. Hong, Y. Kwon, C. Jung, M. Lee, T. Kim, and D. I. D. Cho, A new microfabrication method for ion-trap chips that reduces exposure of dielectric surfaces to trapped ions, J. Microelectromech. Syst. **27**, 28 (2018).

[49] S. Ragg, C. Decaroli, T. Lutz, and J. P. Home, Segmented ion-trap fabrication using high precision stacked wafers, Rev. Sci. Instrum. **90**, 103203 (2019).

[50] J. P. Home, M. J. McDonnell, D. J. Szwer, B. C. Keitch, D. M. Lucas, D. N. Stacey, and A. M. Steane, Memory coherence of a sympathetically cooled trapped-ion qubit, Phys. Rev. A **79**, 050305 (2009).

[51] G. Baggio, F. Ticozzi, P. D. Johnson, and L. Viola, Dissipative encoding of quantum information, arXiv:2102.04531.

[52] I. Rojkov, D. Layden, P. Cappellaro, J. Home, and F. Reiter, Bias in error-corrected quantum sensing, arXiv:2101.05817.

[53] D. Gottesman and I. L. Chuang, Demonstrating the viability of universal quantum computation using teleportation and single-qubit operations, Nature (London) **402**, 390 (1999).

[54] J. R. Maze, A. Gali, E. Togan, Y. Chu, A. Trifonov, E. Kaxiras, and M. D. Lukin, Properties of nitrogen-vacancy centers in diamond: The group theoretic approach, New J. Phys. **13**, 025025 (2011).

[55] A. Mitra, M. J. Martin, G. W. Biedermann, A. M. Marino, P. M. Poggi, and I. H. Deutsch, Robust Mølmer-Sørensen gate for neutral atoms using rapid adiabatic Rydberg dressing, Phys. Rev. A **101**, 030301(R) (2020).